Superlattice dislocations and magnetic transition in Pt_3Fe alloy with the $L1_2$-type ordered structure

1990 J. Phys.: Condens. Matter 2 2133

(http://iopscience.iop.org/0953-8984/2/9/003)

J. Phys.: Condens. Matter 2 (1990) 2133–2142. Printed in the UK

Superlattice dislocations and magnetic transition in Pt_3Fe alloy with the $L1_2$-type ordered structure

S Takahashi† and Y Umakoshi‡

† Faculty of Engineering, Iwate University, Morioka 020, Japan

‡ Department of Materials Science and Engineering, Faculty of Engineering, Osaka University, Suita 565, Japan

Received 6 February 1989, in final form 13 July 1989

Abstract. The magnetic susceptibility was measured in plastically deformed 25.6 at.% Fe–Pt single crystals. The susceptibility decreases considerably as a result of a small strain ε of 1.3% and at the same time spontaneous magnetisation appears. The spontaneous magnetisation increases with increasing plastic deformation. On cooling, the spontaneous magnetisation increases rapidly near the Néel temperatures and has a local maximum at 150 K. The dislocation density and its distribution were also observed by transmission electron microscopy. Superlattice dislocations are distributed making a pair. Near the anti-phase boundary between two superpartials, Fe atoms occupy the face-centred sites and couple ferromagnetically. The relation between the spontaneous magnetisation and the dislocation density is discussed using a simple localised moment model. It is shown that the ferromagnetic transition is extended as far as about twentieth nearest neighbour from the anti-phase boundary. The influence of the ferromagnetic clusters on their neighbouring Fe atoms is extended as far as 10^2 nm and the Fe atoms change to being superparamagnetic. This long-distance influence and the local maximum of spontaneous magnetisation should be explained from the viewpoint of the itinerant-electron model.

1. Introduction

Pt_3T (T ≡ Mn, Co and Fe) has the $L1_2$-type ordered structure. Pt_3Mn and Pt_3Co are ferromagnetic but Pt_3Fe is antiferromagnetic. The reason for these different magnetic structures has been studied experimentally and theoretically. In particular, the magnetic properties of Pt_3Fe have been investigated since the study of Crangle (1959) and Bacon and Crangle (1963). The Pt_3Fe alloy displays two kinds of antiferromagnetic phase; on cooling, $(\frac{1}{2}, \frac{1}{2}, 0)$- and $(\frac{1}{2}, 0, 0)$-type antiferromagnetic structures appear at 170 K ($= T_{N1}$§) and at about 100 K ($= T_{N2}$§), respectively. The spin-wave dispersion relations in Pt_3Fe were investigated by neutron scattering and interpreted in terms of the Heisenberg model with direct exchange interactions between localised magnetic moments (Kohgi *et al* 1978, Kohgi and Ishikawa 1980). Recently it was theoretically shown by Kulikov *et al* (1985) that the particular magnetic structures in Pt_3Fe are associated with the spin-density-wave instability in the electron band system. The static susceptibility function calculated by Kulikov *et al* shows good agreement with that obtained from

§ The subscript i in T_{Ni} is substituted in an earlier paper (Takahashi and Umakoshi 1988).

0953-8984/90/092133 + 10 $03.50

neutron scattering measurements by Kohgi and Ishikawa (1980). It was found that the antiferromagnetic structures are very sensitive to plastic deformation and that they change into ferromagnetic and/or paramagnetic structures as a result of a small strain (Takahashi and Umakoshi 1988). It is of our interest to study the reason why only Pt_3Fe alloys behave antiferromagnetically and to explore whether these antiferromagnetic structures are stable or not.

The magnetic transition from antiferromagnetic to ferromagnetic structures occurs as a result of strong cold work such as filing or machining; Pt_3Fe alloy, which shows antiferromagnetic ordering in the fully $L1_2$-ordered state, becomes strongly ferromagnetic even at room temperature after deformation (Bacon and Crangle 1963). Since early work by Crangle (1959), the magnetic anomaly due tc plastic deformation has been only qualitatively explained with consideration of the effect of the atomic arrangements and/or the configuration of atom–atom pairs before and after deformation. The spontaneous magnetisation is induced by plastic deformation and it is represented as a function of the dislocation density on a basis of the localised-moment model (Takahashi and Ikeda 1983). One of the purposes of the present study is to examine experimentally the qualitative relation between the spontaneous magnetisation and the dislocation density.

When Pt_3Fe alloys are plastically deformed, the number of ferromagnetic Fe atoms in the antiferromagnetic ordered state can be changed and controlled as a function of dislocation density. Therefore, the present method is very useful for studying the magnetic properties in the $L1_2$-type ordered structure without composition change. Very small parts of a ferromagnetic state or small groups of ferromagnetic Fe atoms can be introduced into the antiferromagnetic ordered states by plastic deformation. Generally the localised moment model is unable to give a reasonable explanation for the coexistence of ferromagnetic and antiferromagnetic ordered states (Moriya and Usami 1977). The possibility of the coexistence of antiferromagnetism and ferromagnetism will also be discussed.

2. Experimental procedure

Rectangular prisms (50 mm × 3 mm × 3 mm) were cut from a single-crystal rod of 25.6 at.% Fe–Pt alloy. They were annealed at 1300 K for 1 d in vacuum and then cooled very slowly at 30 K d^{-1} to 870 K to obtain a high degree of $L1_2$-type long-range order. They were tested in tension at room temperature with an Instron-type machine. The stress axis is referred to the standard unit triangle (figure 1). Magnetic measurements were carried out on a balance suitable for measuring the susceptibility of paramagnetic specimens at temperatures from 77 K to room temperature. Thin-foil specimens for electron microscopy were cut first from the deformed specimens by spark machining and finally thinned by ion sputtering. The thin foils were examined in an H-800 electron microscope operating at 200 kV. The $L1_2$-type ordered structure in Pt_3Fe alloy was confirmed by electron diffraction observations.

3. Experimental results

3.1. Magnetic measurements

In the alloy before plastic deformation, to which figure 1 refers, the isothermal magnetic measurements were carried out in the range of magnetic field strengths between 8×10^4

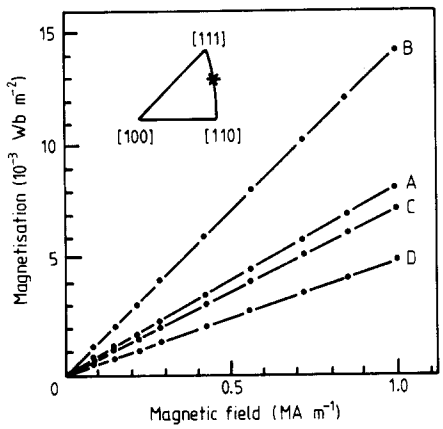

Figure 1. The variation in magnetisation with applied magnetic field at different temperatures for an undeformed 25.6 at.% Fe–Pt single crystal: line A, 77 K; line B, 105 K; line C, 165 K; line D, 273 K. The orientations of the tensile axis and of the applied field are the same and shown in the standard unit triangle.

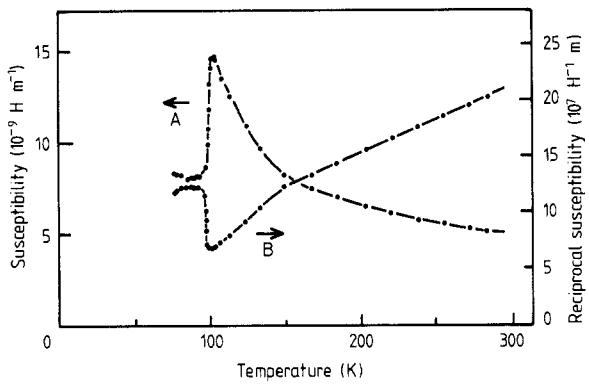

Figure 2. The variations in susceptibility (curve A) and reciprocal susceptibility (curve B) with test temperatures for the undeformed alloy containing 25.6 at.% Fe.

and 9.8×10^5 A m^{-1}. No significant variation in the susceptibility with magnetic field was detected in the undeformed specimens, implying that no ferromagnetic state was present. The magnetic field was applied parallel to the stress axis, as shown in the standard unit triangle. Magnetic measurements were carried out for other orientations but the isothermal magnetic curves were found to be independent of the crystal orientation. The magnetic susceptibility was determined by a least-squares fit to the isothermal magnetic data. The temperature dependences of susceptibility and reciprocal susceptibility are shown in figure 2. A minimum in the reciprocal susceptibility curve is observed near 100 K in agreement with the work of Crangle (1959). The Néel temperature can be estimated to be 105 K from the peak in the susceptibility curve, corresponding to the $(\frac{1}{2}, 0, 0)$ antiferromagnetic structure. The same variation in reciprocal susceptibility with temperature as found by Bacon and Crangle (1963) shows that there exist two types of antiferromagnetic structure with 105 and 165 K as the Néel temperatures. At temperatures above 165 K the magnetic susceptibility behaves in accordance with the Curie–Weiss law but near 165 K the linear relation in the reciprocal susceptibility shows a discontinuity. The Curie constant in the present specimen is also the same as that found by Crangle (1959) within 10%.

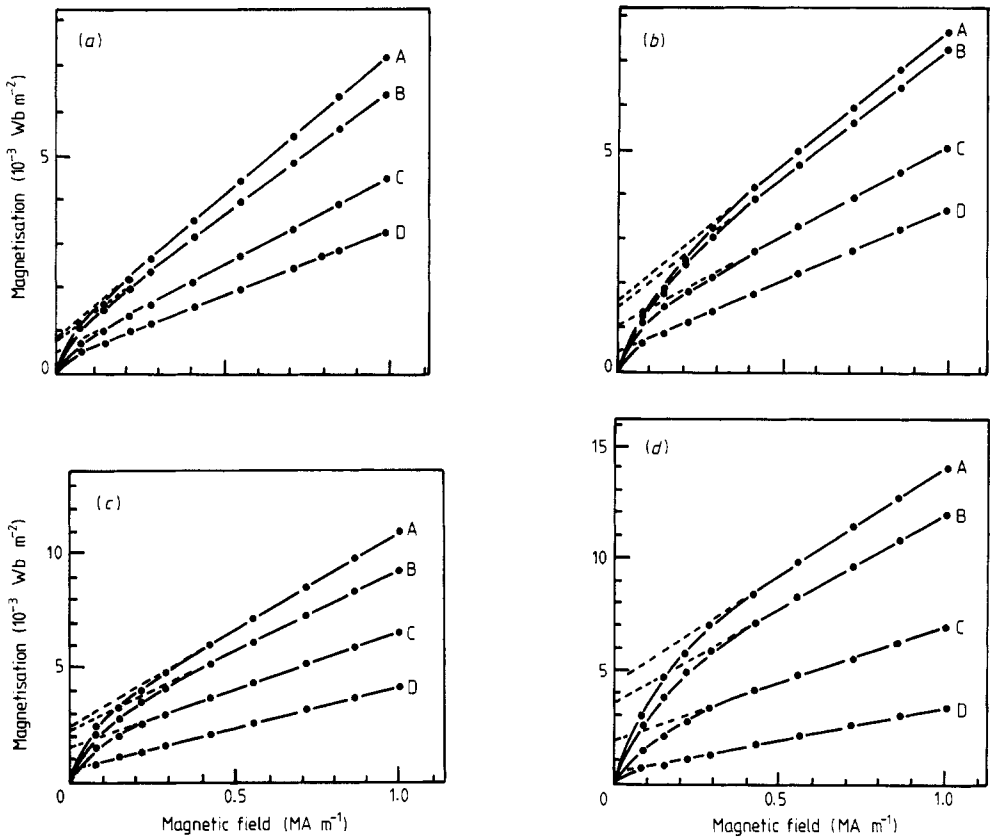

Figure 3. The variation in magnetisation with applied magnetic field at different temperatures for 25.6 at.% Fe–Pt single crystals after plastic deformation at (*a*) $\varepsilon = 1.3\%$, (*b*) $\varepsilon = 6.5\%$, (*c*) $\varepsilon = 11.6\%$ and (*d*) $\varepsilon = 22\%$: lines A, 77 K; lines B, 105 K; lines C, 165 K; lines D, 273 K).

Figure 3 shows the isothermal magnetisation curves for the specimens deformed to 1.3, 6.5, 11.6 and 22% tensile strains (ε). After a small plastic deformation with $\varepsilon = 1.3\%$, the magnetisation decreases at every temperature in comparison with the undeformed results (see figure 1) and then increases gradually with increasing plastic strain. The linearity of magnetisation deviates in the low-field range. The susceptibility is obtained from the linear part of magnetisation curves and in the 22%-strained specimen, for example, the linearity is obtained above 4.4×10^5 A m^{-1} at 77 K. The spontaneous magnetisation is obtained by the usual procedure of extrapolating the linear parts of magnetic isothermals back to zero magnetic field. The extrapolation is shown by the broken lines in figure 3.

The reciprocal susceptibility is also plotted as a function of temperature in figure 4. The reciprocal susceptibility above 170 K increases linearly with increasing temperature, but some deviation from the linearity is observed near T_{N1} for the deformed specimens. The slopes of reciprocal susceptibility lines above T_{N1} are the same in the specimens with $\varepsilon = 0\%$ and $\varepsilon = 1.3\%$ (see figure 1 in Takahashi and Umakoshi (1988)). The slope becomes steeper with increasing plastic deformation. The paramagnetic Néel temperature is −65 K for the undeformed specimen and decreases markedly to −315 K

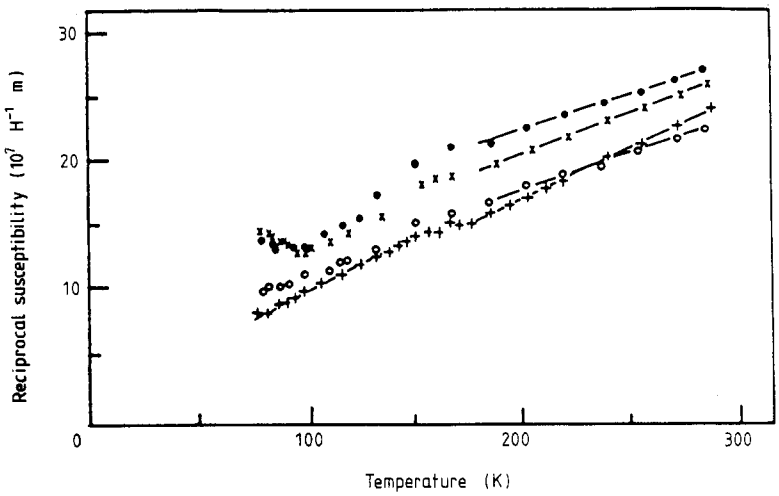

Figure 4. The variation in reciprocal susceptibility with temperature for the alloy containing 25.6 at.% Fe after plastic deformation: ●, $\varepsilon = 6.5\%$; ×, $\varepsilon = 10\%$; ○, $\varepsilon = 11.6\%$; +, $\varepsilon = 22\%$.

for the specimen with $\varepsilon = 1.3\%$. The paramagnetic Néel temperature increases with increasing plastic strain and becomes −15 K for the specimen deformed to 22%. The deviation from linearity in the reciprocal susceptibility near T_{N1} and T_{N2} becomes smaller with increasing plastic strain, especially near T_{N2}. In the specimen with $\varepsilon = 22\%$, a small deviation can be admitted only at T_{N1} and the deviation near T_{N2} disappears.

The variations in spontaneous magnetisation with temperature are shown in figure 5. The uncertainties in spontaneous magnetisation due to the instability of test temperature are shown by the error bars. The spontaneous magnetisation depends on temperature but the relation is plotted only for the specimens with more than 5.6% strain because of the small dependence for the specimens with less than 5.6% strain. The spontaneous magnetisation increases with decreasing temperature. In the specimens with $\varepsilon = 22\%$ and $\varepsilon = 11.6\%$, two impressive features are revealed. One is the rapid change in spontaneous magnetisation near T_{N1} and T_{N2} and the other is that the spontaneous magnetisation has a local maximum near 150 K.

3.2. Electron microscopy observation

The dissociation of superlattice dislocations in the $L1_2$-type ordered structure was studied by Marcinkowsky *et al* (1961). In the Pt_3Fe alloy the order–disorder transformation takes place somewhere between 973 and 1037 K (Kussmann and Rittberg 1950), and therefore the anti-phase boundary (APB) energy on {111} planes is low. It is supported by the dark-field image of the anti-phase domain (APD) boundary as seen in figure 6(*a*). A $[\bar{1}01]$ superlattice dislocation in this alloy is expected to be rather widely separated into two $\frac{1}{2}[\bar{1}01]$ superpartials coupled by a ribbon of APB. The APB width is seen to be about 13 nm from the high-magnification photograph in figure 6(*b*). The individual $\frac{1}{2}[\bar{1}01]$ superpartials may be dissociated into two Shockley partials, but dissociation cannot be observed since the complex stacking fault energy is high.

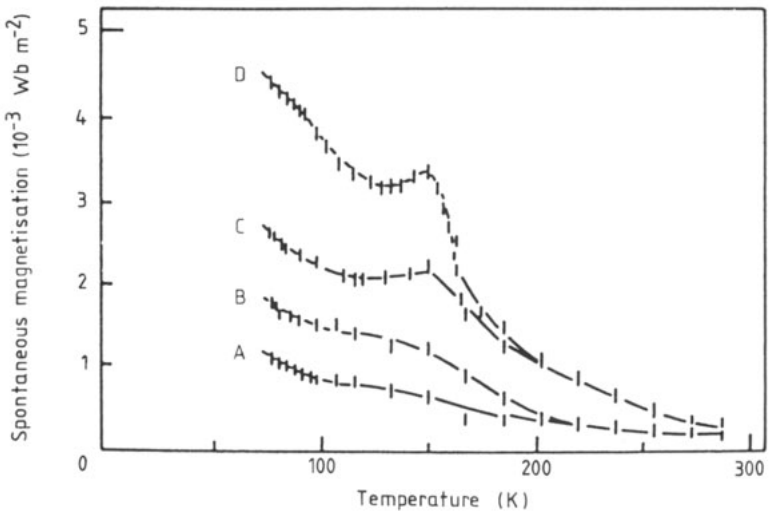

Figure 5. The variation in the spontaneous magnetisation due to plastic deformation with temperature: curve A, $\varepsilon = 5.6\%$; curve B, $\varepsilon = 10\%$; curve C, $\varepsilon = 11.6\%$; curve D, $\varepsilon = 22\%$.

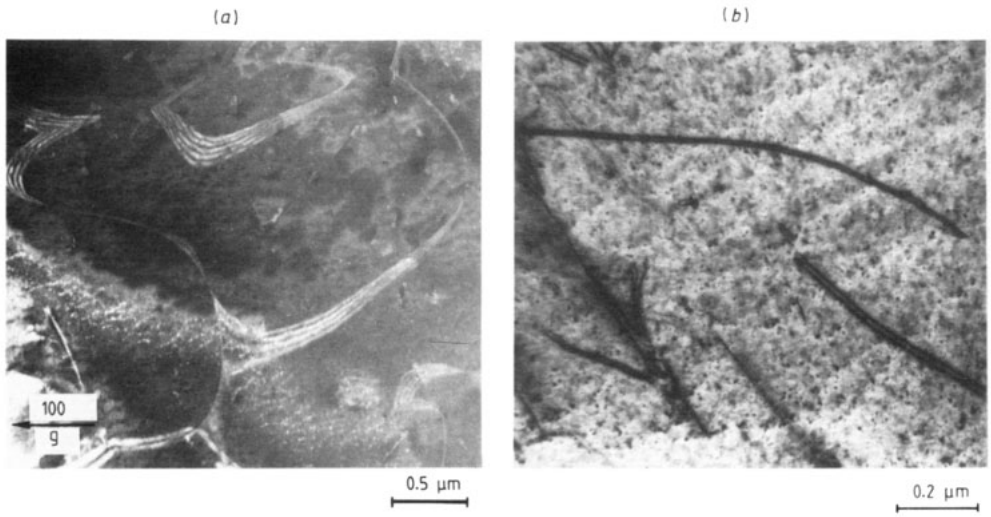

Figure 6. (*a*) Dark-field image of the APD boundary of a 25.6 at.% Fe–Pt single crystal. (*b*) The dissociation of a $[\bar{1}01]$ superlattice dislocation in a 25.6 at.% Fe–Pt single crystal deformed to 5.6% strain.

Figures 7(*a*), 7(*b*), 7(*c*) and 7(*d*) are the electron micrographs of specimens with ε values of 5.6%, 6.5%, 7.9% and 11.6%, respectively. The Burgers vector and the glide plane of these dislocations are confirmed to be $(a/2)\langle 110\rangle$ and $\{111\}$, respectively. Almost all the dislocations are in pairs. The distribution of dislocations is fairly uniform and the mean distance between superlattice dislocations is $(4 \pm 1) \times 10^2$ nm in the 1.3%-strained specimen and decreases with increasing plastic strain. The dislocation density was

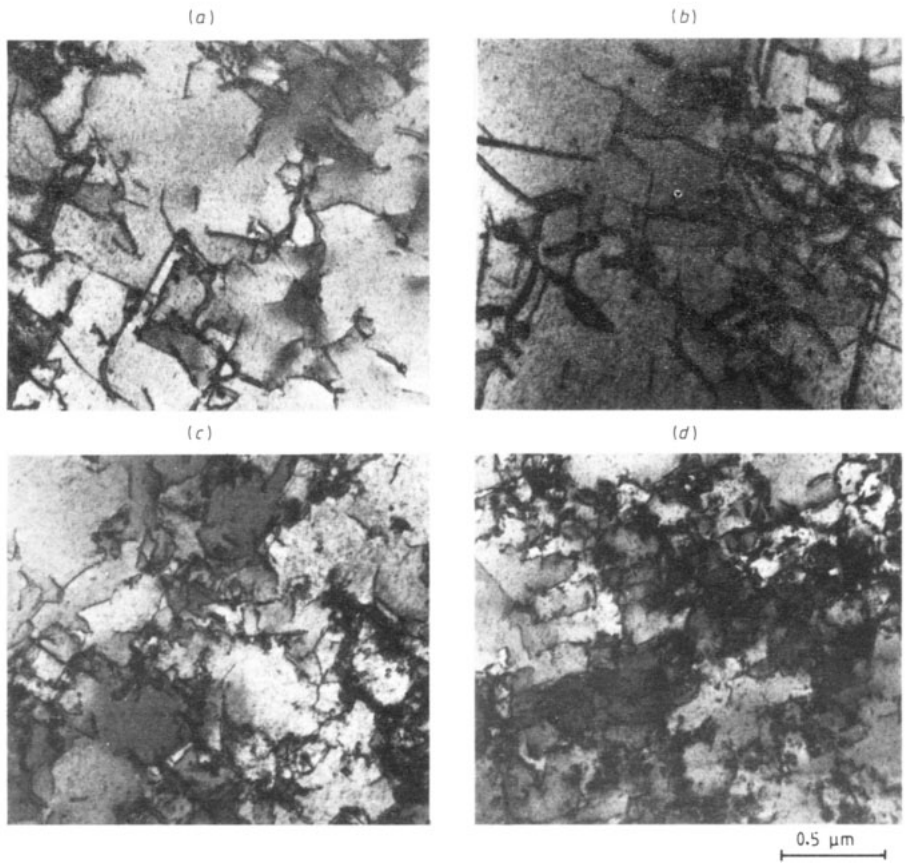

Figure 7. The electron micrographs of 25.6 at.% Fe–Pt single crystals deformed plastically: (*a*) $\varepsilon = 5.6\%$; (*b*) $\varepsilon = 6.5\%$; (*c*) $\varepsilon = 7.9\%$; (*d*) $\varepsilon = 11.6\%$.

measured by counting the intersection of dislocation lines with straight lines drawn at random on photographic films. The dislocation density increases with increasing strain, from 10^8 to 10^{10} cm^{-2}. It contains about 30% experimental errors depending on the ambiguity of the thickness of specimens.

4. Superlattice dislocations and magnetic transition

$[\bar{1}01]$ superlattice dislocations are usually induced in Pt_3Fe by plastic deformation. To be more exact, a $\frac{1}{2}[\bar{1}01]$ leading superpartial dislocation creates an APB on the {111} glide plane after it has slipped and it is stable to make a pair with another $\frac{1}{2}[\bar{1}01]$ superpartial dislocation. Fe and Pt atoms are replaced at different occupation sites on the APB. Excluding APB stripes, the crystal structure is conserved to be the $L1_2$-type structure. Fe atoms occupy the corner sites and they are located at the second-nearest neighbour in the $L1_2$-type structure (figure 8(*a*)). Near the APB, however, they are located at the first-nearest neighbour (figure 8(*b*)). The number of Fe atoms at the face-centred sites is represented as a simple function of dislocation density ρ (Takahashi and Ikeda 1983).

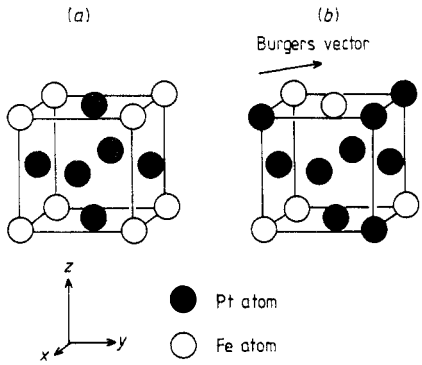

Figure 8. Atomic arrangement for ideal stoichiometric Pt_3Fe: (*a*) atomically ordered states; (*b*) after the $(a/2)$ $[\bar{1}10]$ slip over the (111) glide plane. The APB distributes over the (111) glide plane.

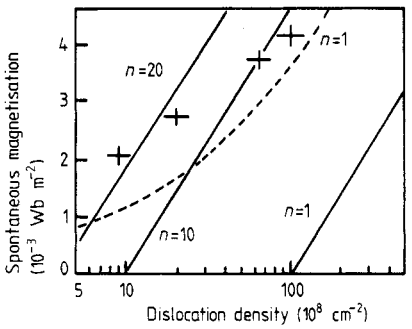

Figure 9. The spontaneous magnetisation induced by plastic deformation versus dislocation density ρ: +, experimental results; ———, calculated according to equation (3), when superlattice dislocations are distributed as pairs; – – – –, calculated according to equation (3) when superlattice dislocations are independent and free from the attractive force due to the APB; *n* indicates the degree of magnetic influence of the ferromagnetic Fe atoms at the irregular sites.

According to the electron micrographs, superlattice dislocations are distributed, making pairs which are called A-type superlattice dislocations in this paper. Then the number of Fe atoms per unit volume is given as

$$N' = (S^2 r_0/\sqrt{3}a^2)\rho \tag{1}$$

where S is the degree of order, a is a lattice constant and r_0 ($= 13$ nm) is the separation of superpartial dislocations or the width of the APB stripe.

Another type of superlattice dislocation is possible, i.e. one which is distributed independently and is free from the attractive force of the APB. This type would appear mainly in the advanced deformation stage and is called a B-type superlattice partial dislocation. For B-type superlattice partial dislocations, the number of Fe atoms becomes

$$N' = (S^2/\sqrt{3}a^2)\sqrt{\rho}. \tag{2}$$

The experimental results show that Fe atoms at the face-centred sites near APB couple ferromagnetically. If the magnetic transition from antiferromagnetism to ferromagnetism is extended as far as the nth-nearest-neighbour distance from the APB, the number N of ferromagnetically coupled Fe atoms is nN'. The net spontaneous magnetisation of the plastically deformed Pt_3Fe alloy at 0 K can be written as

$$M(0) = N\mu_{Fe} \tag{3}$$

where μ_{Fe} is the magnetic moment of the Fe atom at the face-centred site.

The above relations between spontaneous magnetisation and the dislocation density are shown in figure 9 in comparison with the experimental results. Here $\mu_{Fe} = 4.0\mu_B$

(Bacon and Crangle 1963) and $S = 1$ in equations (1) and (2) are adopted in the calculated results and, for the spontaneous magnetisation, the values at 77 K are adopted in the experimental results. The uncertainties of the dislocation density are shown by the error bars. The calculated results are shown by the full lines and a broken curve for A- and B-type superlattice dislocations, respectively. For B-type superlattice dislocations, the calculated result agrees well with the experimental result without consideration of the effect of the long-distance magnetic influence. However, B-type superlattice dislocations could not be observed, especially in the initial deformation stage. A-type superlattice dislocations predominate in the present specimens.

5. Discussion

The comparison of experiment and calculation for A-type superlattice dislocations as shown in figure 9 suggests that Fe atoms near the APB exert a magnetic influence on their neighbouring Fe atoms as far as the tenth- to twentieth-nearest neighbour and make them ferromagnetic. In fact the magnetic influence would extend farther than these nearest-neighbour distances, since the magnitude of spontaneous magnetisation at 0 K would be larger than that at 77 K and the magnetic moment of Fe atoms would be 3.3 μ_B or 2.2 μ_B. The different values of n which depend on the deformation stage do not occur when there is an overlapping distribution of APB stripes. The mean distance between APB stripes in the highest-density part is still greater than 10 nm (see figure 7), which is much larger than the twentieth-nearest neighbour distance. This distance is large enough for the APB stripes not to overlap each other.

However, the different values of n can be explained if B-type superlattice dislocations appear at the advanced deformation stage, although their density is low. The width of the APB stripe in B-type superlattice dislocations is much larger than that of A-type dislocations, and then N' increases sharply as plastic deformation advances, while the magnetic interaction distance does not change. Therefore, n becomes small apparently.

Another explanation for the different values of n is possible. A thermally induced APD exists before plastic deformation as shown in figure 6(a). At the initial deformation stage, dislocations nucleate. slip on the {111} plane and cross the thermally induced APD boundary. This dislocation-crossing effect increases the area of the APB glide plane, and this effect would become small at the advanced deformation stage where dislocations are pinned at the obstacles and hardly slip over the long distances. n apparently has a large value in the initial deformation stage. In fact the different geometrical morphologies of the APB and APD may induce the change in n-value at various deformation stages. The mutual interaction of the thermally induced APD and the slip-induced APB may contribute to extending the effective distance. It is difficult to distinguish between the effects of the APD and B-type superlattice dislocations only from the present experiment. Both effects would contribute to the present phenomenon.

The magnetic susceptibility usually depends on the atomic structure. Some of the Fe atoms are displaced to the face-centred sites by plastic deformation but they are very few. Almost all Fe and Pt atoms remain in the same atomic arrangement as before deformation. The magnetic susceptibility, however, decreases considerably as a result of plastic deformation. The decrease in susceptibility results from the long-distance influence which the ferromagnetic clusters exert on the neighbouring Fe atoms. The mean distance between APB stripes is greater than 3×10^2 nm in the 1.3%-strained specimen. Thus the influence of the ferromagnetic cluster extends to as far as

1.5×10^2 nm at least. The long-distance influence is difficult to explain in terms of a simple Heisenberg model with direct exchange interaction in sixth-neighbour spheres (Kohgi and Ishikawa 1980). The antiferromagnetic structure still remains in the initial deformation stage. In the 22%-strained specimen, however, the reciprocal susceptibility becomes linear near T_{N2}, and then the $(\frac{1}{2}, 0, 0)$-type antiferromagnetic structure is destroyed. The increase in paramagnetic Néel temperature with increasing plastic strain also favours a magnetic transition from the antiferromagnetic structure to the paramagnetic and ferromagnetic structures.

The magnetic moment of the Fe atom in the 0%- or 1.3%-strained specimen is found to be $(5.3 \pm 0.1)\mu_B$ from the Curie–Weiss law, where Pt atoms carry a zero magnetic moment. The magnetic moment in the specimens with a higher strain becomes smaller and is $(4.2 \pm 0.1)\mu_B$ in the 22%-strained specimen. These values are from twice to two-and-a-half times the usual iron moment of $2.2\mu_B$. These large magnetic moments show the limit of the localised-moment model (Moriya 1979).

A distinct local maximum is recognised near 150 K in the spontaneous magnetisation–temperature curve. This phenomenon favours itinerant-electron magnetism such as the self-consistent renormalisation theory of spin fluctuations (Moriya 1979). Evidence of itinerant antiferromagnetism was observed in the study of Bacon and Crangle (1963); the local maximum is observed near 120 K in the neutron diffraction intensity from the $(\frac{1}{2}, \frac{1}{2}, 0)$ antiferromagnetic ordering.

Acknowledgments

It is a pleasure to acknowledge the provision of single crystals by Dr S Hayashi (Institute for Materials Research, Tohoku University), and the technical assistance of Mr Y Sakanoue.

References

Bacon G E and Crangle J 1963 *Proc. R. Soc.* A **272** 387
Crangle J 1959 *J. Phys.* **20** 435
Kohgi M and Ishikawa Y 1980 *J. Phys. Soc. Japan* **49** 985
Kohgi M, Ishikawa Y and Radhakrishna P 1978 *Solid State Commun.* **27** 409
Kulikov N I 1985 *J. Phys. F: Met. Phys.* **15** 1139
Kulikov N I, Kulatov E T and Yakhimovich S I 1985 *J. Phys. F: Met. Phys.* **15** 1127
Kussmann A and Rittberg G V 1950 *Z. Metallk.* **42** 470
Marcinkowski M J and Brown N 1961 *Acta Metall.* **9** 764
Moriya T 1979 *J. Magn. Magn. Mater.* **14** 1
Moriya T and Usami K 1977 *Solid State Commun.* **23** 935
Takahashi S and Ikeda K 1983 *J. Phys. Soc. Japan* **52** 2772
Takahashi S and Umakoshi Y 1988 *J. Phys. F: Met. Phys.* **18** L257